# Transient Responses Analysis of Some Ultra-Wideband Fliters in the Presenceof Wideband Electromagnetic Pluses

*Qi-Feng Liu[1], Zheng Jiang[2], Wen-Yan Yin[2], Chong-Hua Fang[1], and Jing-Wei Liu[3]*

[1] China Ship Development and Design Centre, Science and Technology on Electromagnetic Compatibility Laboratory, Wuhan, China, emclqf@126.com
[2] Center for Optical and EM Research (COER), Zhe Jiang University, Hangzhou, 310058, China
[3] Wuhan Wuda Jucheng Strengthening Industrial Co. Ltd, Wuhan, China

## Abstract

It is well known that intentional or unintentional electromagnetic interference can impact on microwave circuits or systems to make them improper functionality, and in this paper, we analysis the transient responses of two ultra-wideband (UWB) filters under a high-power EMP. Based on a modified FDTD method, numerical calculation is performed to show the EMP interference impacting on the S-parameters of UWB filters which are usually used in the wideband integration of communication circiuts and systems. The statistical analysis provides a new procedure for a confidence determination of the interference behavior parameters.

## 1. Introduction

Intentional electromagnetic interference (IEMI) refers to "intentional malicious generation of electromagnetic energy introducing noise or signals into electrical and electronic systems, thus disrupting, confusing, or damaging these systems for terrorist or criminal purposes" [1]. Such an IEMI can be generated by a high-power microwave source, such as high-power ultra-wideband pulse antenna [2], [3].

On the other hand, it is known that the Federal Communications Commission (FCC) released the unlicensed use of ultra-wideband wireless standard in 2002 [4], and many researchers have started to explore various UWB components and systems, in particular for the bandpass filters (BPFs) with large fractional bandwidths (FBWs) driven by wide applications of indoor/outdoor ultra-wideband (UWB) communication systems. Physically, an ultra-wideband communication system could be easily disturbed by an ultra-wideband EMP, which should be paid more attention for their certain applications.

To the best of our knowledge, two types of UWB filters have been proposed in [5] and [6] more recently. For example, a novel compact UWB parallel coupled BPF is proposed in [5] using single CPW resonator whose length is only quarter-wavelength and coupled to two microstrip open-circuited stubs in parallel on the other side of a substrate. In [6], a compact ultra-wideband bandpass filter with improved upper stopband is proposed. However, our study will focus on anglicizing their transient responses when they are disturbed by a high-power electromagnetic(HPEM) interference.

In this paper, we restrict using the FDTD method to investigate transient responses of bandpass filters illuminated by an EMP. In Section II, the geometry of filters is provided. In Section III, the theory of FDTD and the definition of S-parameters and breakdown failure error of S-parameter are shown in detail. In Section IV, statistical analysis of parasitic studies is performed to demonstrate the effects of the external HPEM interference on S-parameters of the UWB filters. Some conclusions are drawn in Section V.

## 2. Problem Definition

A 3-D architecture of a UWB filter is shown in Fig. 1(a), which is constructed on single-layer dielectric substrate with a thickness of $h$ [5]. It has a symmetrical structure; and in its middle, a quarter-wavelength CPW resonator with a width of $W_2$ and a length of $L_2$ is formed on the bottom side of the substrate. The dimensions for the CPW structure are $W_2$ = 2.4 mm and $s$ = 0.2 mm, which results in characteristic impedance of 58 Ω on a 0.508-mm thick substrate with a relative dielectric constant of 3.05. The size of the CPW resonator is $8.6\times2.4$ mm2. On the top side of the substrate, two parallel microstrip open-circuited stub lines of $W_1$ wide and $L_1$ long are coupled to the CPW resonator through the dielectric substrate. The two open-circuited stubs, separated by a gap of g, are connected to 50- input/output (I/O) feed lines having a width of $W_0$ . For these results, the filter has fixed dimensions (also refer to Fig. 1) of $W_0$ = 1.2 mm, $W_1$ = 0.8 mm, $L_1$ = 6.2 mm, $W_2$ = 2.4 mm, $L_2$ = 8.6 mm and $s$ = 0.2 mm. This is a very compact filter only occupying a circuit arera about $0.25\lambda\times0.08\lambda$ , where $\lambda$ is the guided wavelength at the center frequency.

978-1-4673-5225-3/14/$31.00 ©2014 IEEE

Fig.1(b) also shows the schematic of the 2-D UWB bandpass filter, which has a square slot-line resonator(SLR) with slot-line stub etched in the ground plane and modified T-shaped feed lines. The demension of the filter is followed: $W_1 = 1.2$ mm, $W_2 = 0.3$ mm, $W_3 = $=0.4 mm, $L_1 = $=3.6 mm, $L_2 = 8.95$ mm, $S = 0.9$ mm, $D = 8.35$ mm, and $h = 0.381$ mm thick Rt/duroid 5880 substrate having dielectric constant εr=2.2 has been used. Filter occupying area is 0.26λg × 0.26λg, λg being the microstrip line guided wavelength at 6.85GHz.

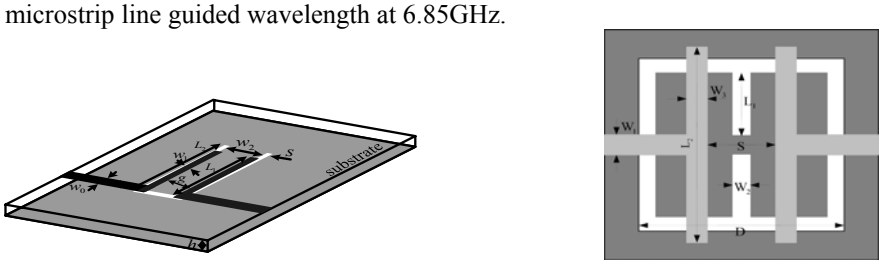


(a) (b)

Fig. 1. The UWB microstrip/CPW filters

The incident EMP wave vector is described by

$$\vec{k}_{inc} = \vec{e}_x s\sin\theta\ \cos\varphi\ + \vec{e}_y \sin\theta\ \sin\varphi\ + \vec{e}_z \cos\theta \tag{1}$$

where $\vec{e}_x$, $\vec{e}_y$, and $\vec{e}_z$ are three unit vectors in the Cartesian coordinate system; the polarizations of the external EMP are determined by the polarization angle $\psi$, and all incident field components are given by

$$E_x^{(inc)} = E^{(inc)}(\sin\varphi\ \cos\psi\ - \cos\theta\ \cos\varphi\ \sin\psi\ ), \tag{2a}$$

$$E_y^{(inc)} = -E^{(inc)}(\cos\varphi\ \cos\psi\ + \sin\varphi\ \cos\theta\ \sin\psi\ ), \tag{2b}$$

$$E_z^{(inc)} = E^{(inc)}\sin\varphi\ \sin\theta\ , \tag{2c}$$

$$H_x^{(inc)} = H^{(inc)}(\sin\varphi\ \sin\psi\ + \cos\varphi\cos\theta\ \cos\psi\ ), \tag{3a}$$

$$H_y^{(inc)} = H^{(inc)}(-\cos\varphi\ \sin\psi\ + \sin\varphi\ \cos\theta\ \cos\psi\ ), \tag{3b}$$

$$H_z^{(inc)} = -H^{(inc)}\sin\theta\ \cos\psi\ . \tag{3c}$$

where $E^{(inc)}$ is described by a triple-exponential function as follows:

$$E^{(inc)} = \sum_{p=1}^{3} \frac{a_i^{(p)}}{b_i^{(p)}\sqrt{\pi/2}} e^{-2\left(\frac{t-t_i^{(p)}}{\tau_i^{(p)}}\right)^2} \tag{4}$$

and the coefficients $a_i^{(p)}$, $b_i^{(p)}$, $t_i^{(p)}$, and $\tau_i^{(p)}$ are obtained according to the pulse waveform.

## 3. The Analysis Theory and Method

***A. the FDTD Method***

The time-dependent Maxwell's curl equations for linear, isotropis, non-dispersive, and lossy media can be written as

$$\nabla\times\vec{H} = \varepsilon\frac{\partial\vec{E}}{\partial t} + \sigma\vec{E}\ ,\ \nabla\times\vec{E} = -\mu\frac{\partial\vec{H}}{\partial t} \tag{5}$$

where $\vec{E}$ and $\vec{H}$ are the electric and magnetic vector fields, respectively. ε is the permittivity, σ is the conductivity, and μ is the permeability of the medium to model. Equations (5) can be solved by the FDTD method based on Yee's grid. According to the leap-frog scheme, the time is discretized into equal time intervals denoted by△t, and then the computation of (5) for the FDTD solution marching from the nth the time step is given by

$$\vec{H}^{n+1/2} = \vec{H}^{n-1/2} - (\Delta t/\mu)\nabla\times\vec{E}^{n}\ ,\ \vec{E}^{n+1} = \frac{\varepsilon-\sigma\Delta t/2}{\varepsilon+\sigma\Delta t/2}\vec{E}^{n} + \frac{1}{\varepsilon+\sigma\Delta t/2}\nabla\times\vec{H}^{n+1/2} \tag{6}$$

According to the basic FDTD notation, the components of vector fields $\vec{E}$ and $\vec{H}$ are computed at different points of the FDTD structure grids. Any component of the fields Fα (t, x, y, z) in a discrete space is denoted as

$$F^{n}{}_{\alpha}(i,j,k) = F^{n}{}_{\alpha}(i\Delta x, j\Delta y, k\Delta z, \Delta t)\ , \tag{7}$$

where α = x , y and z; i, j, k and n are the space and time indexes, △t is the time step, and △x, △y and △z are the space increments along the x-, y- and z- directions, respectively.

***B.Calculation of S-Parameters of Fliters Under Extenal EMP***

The frequency-dependent scattering matrix coefficients are easily calculated from the transient results obtained naturally by the FDTD method:

$$\vec{V}^r = \vec{S}\vec{V}^i \tag{8}$$

where $\vec{V}^r$ and $\vec{V}^i$ are the reflected and incident voltage vectors, respectively, and $\vec{S}$ is the scattering matrix. The FDTD simulation calculates the sum of incident and reflected waveforms. To obtain the incident waveform, the calculation s performed using only the input port microstrip line, which will now be of infinite extent (i.e., from source to far absorbing wall), and the incident waveform is recorded. This incident waveform may now be subtracted from the incident plus reflected waveform to yield the reflected waveform for port 1. The other ports will register only transmitted waveforms and will not need this computation. The scattering parameters si,j may then be obtained by simple Fourier transform of these transient waveforms as

$$s_{i,j} = \frac{FT[v_j(t)]}{FT[v_i(t)]} \tag{9}$$

Note that the reference planes are chosen with enough distance from the circuit discontinuities to eliminate evanescent waves. These distances are included in the definition of the circuit so that no phase correction is performed for the scattering coefficients.

## 4. Results and Analysis

At first, in order to check our FDTD code, we just to calculate the S-parameters of the UWB filter with no external EMP source implemented. The S-parameters are obtained using the Fourier transform at the end of FDTD iteration. Fig. 2 shows the simulated S-parameters of the UWB bandpass filter, as compared with the measurement results given in [5] and [6], respectively; it is obvious that excellent agreements are obtained between them.

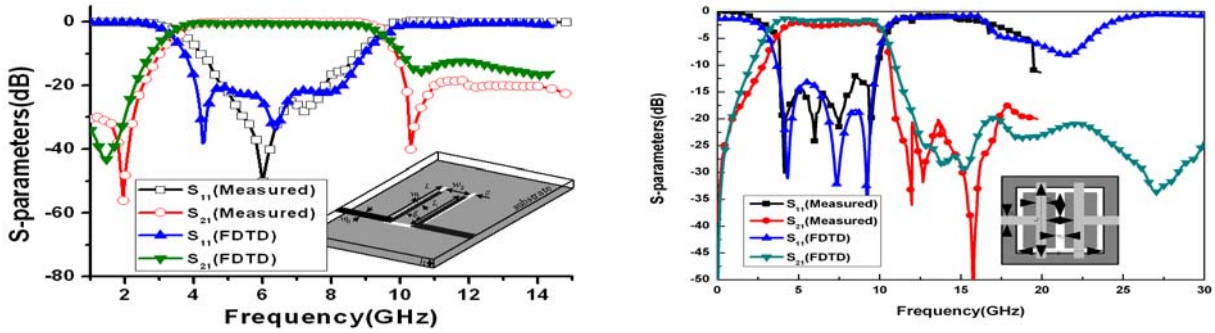


(a) (b)

Fig. 2. Comparisons in the simulated (S) and measured (M) S-parameters of (a) UWB microstrip/CPW filters and (b) slot-line resonator(SLR)filters, respectively.

As the UWB filter is illuminated by a high-power EMP with a spectrum wider than its operational bandwidth. The incident EMP direction is in the direction of $\varphi = 90^o$ and $\theta = 90^o$, with a polarization angle of $90^o$. In the numerical simulation by FDTD method, the Mur [8] absorbing boundary is employed to truncate the computational domain.

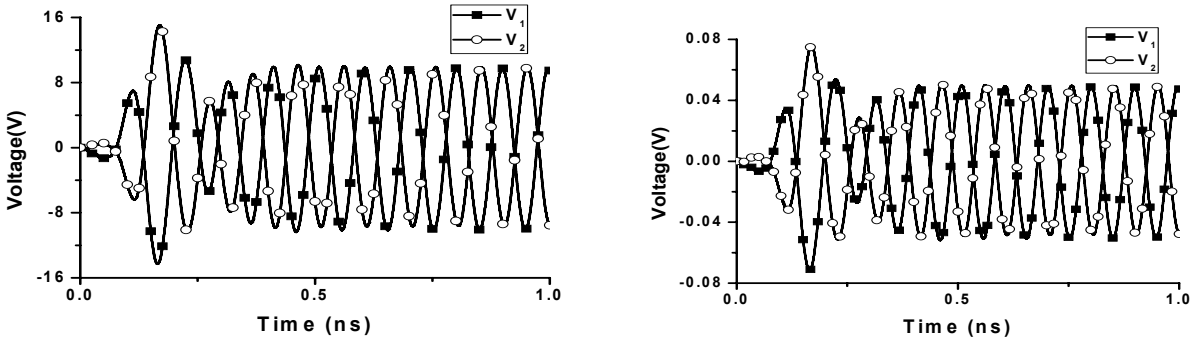


(a) (b)

Fig. 3. The induced voltages at the input/output ports of the filter (a) with no shielding enclosure implemented; and (b) shielded by a metallic enclosure.

In our simulation, the output and input ports are terminated with 50Ω matched loads, and the induced voltages at the input and output ports of Fig.1 (a) are plotted in Fig. 3(a). It is found that the external high-power wideband EMP can induce as high as 15.8 V and 11.6 V voltages at its output and input ports, respectively, which is much higher than that of the normal input signal voltage. Then, we assume both filters are shielded by a metallic enclosure, respectively. Under such circumstances, the inner input signal magnitude will be much smaller than that of the external EMP (about decrease 23 dB in magnitude). In Fig. 3(b), it is shown that much lower voltage signals are reduced at two output ports, as compared with those in Fig. 3(a), respectively. Also, numerical results for the case of no external EMP source implemented are plotted in Fig.4 for comparison. Certainly, both ultra-band wideband filters can be disturbed by the external EMP seriously, in particular for the $S_{11}$ -parameter.

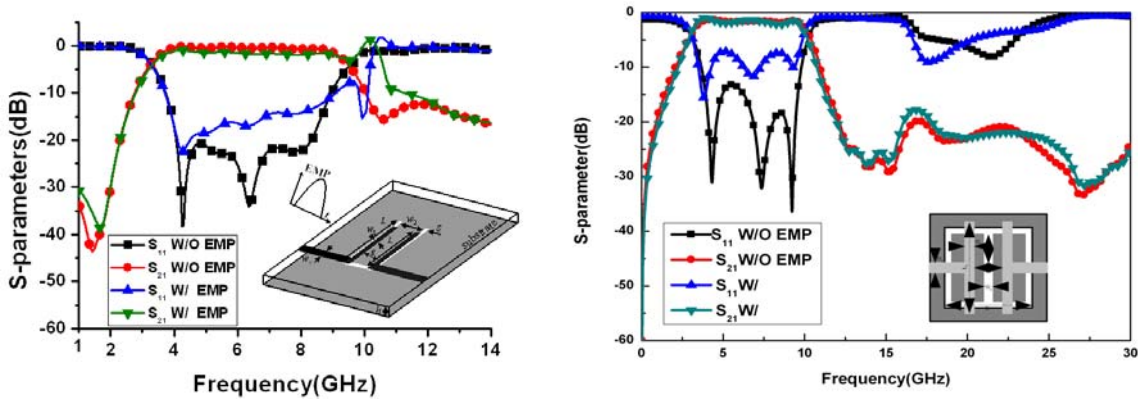


(a) (b)

Fig.4. The S-parameters of the ultra-band bandpass filters in an metallic enclosure, respectively; W/O: no external EMP source introduced, and W: illuminated by an EMP.(a) the UWB microstrip/CPW filters, and (b) the UWB bandpass with improved Upper stopband.

## 5. Conclusion

The FDTD method is implemented to characterize EM interference in UWB filters caused by an external EMP. Our FDTD code is very efficient in computation, and the S-parameters characteristics are captured for different geometrical and physical parameters of the structure. The investigation of susceptibility of S-parameters illuminated by UWB pusles shows that different signal on the susceptibility is very large and different. Although metallic shielding is often an effective way to protect circuit systems against external EMI, better protection methods should be further implemented and explored.

## 6. References


1. W. A. Radasky, C. E. Baum, and M. W. Wik, “Introduction to the special issue on high-power electromagnetics (HPEM) and intentional electromagnetic interference (IEMI),” IEEE Trans. Electromagn. Compat., vol. 46, no. 3, pp. 314-321, 2004.

2. F. Sabath, M. Backstrom, B. Nordstrom, D. Serafin, A. Kaiser, B. A. Kerr, and D. Nitsch, “Overview of four European high-power microwave narrow-band test facilities, ” IEEE Trans. Electromagn. Compat., vol. 46, no.3, pp. 329-334, Aug. 2004.

3. W. D. Prather, C. E. Baum, R. J. Torres, F. Sabath, and D. Nitsch, “Survey of worldwide high-power wideband capabilities,” IEEE Trans. Electromagn. Compat., vol. 46, no.3, pp. 335-344, Aug. 2004.

4. Federal Communications Commission, “Revision of part 15 of the commission’s rules regarding ultra-wideband transmission systems,” Tech. Rep., ET-Docket 98–153, FCC02–48, 2002.

5. N. Thomson and J. S. Hong, “Compact ultra-wideband microstrip/coplanar waveguide bandpass filter,” IEEE Microw. Wireless Compon. Lett., vol. 17, no. 3, pp. 184–186, 2007.

6. Priyanka Mondal, Mrinal Kanti Mandal, and Ajay Chakrabarty, “Compact ultra-wideband bandpass filter with improved upper stopband,” IEEE Microw. Wireless Compon. Lett., vol. 17, no. 9, pp. 643–645, 2007.

7. S. V. Georgakopoulos, C. R. Birtcher, and C. A. Balanis,“IRF penetration through apertures: FDTD versus measurements,” IEEE Trans. Electromagnetic Compatibility, vol. 43, no.3, pp. 282-294, Aug. 2001.

8. G. Mur, “Absorbing boundary conditions for the finiter-difference approximation of the time-domain electromagnetic field equations,” IEEE Trans. Electromagn. Compat., vol. 23, no.4, pp. 377-382, Aug. 2004.